

Mechanism of the Reaction between Magnesium Ions and Alizarin Yellow G

BERTA PERLMUTTER-HAYMAN* and RUTH SHINAR

Received August 9, 1976

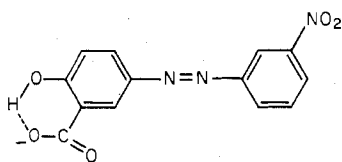
AIC60573U

The kinetics of the reaction between Mg^{2+} and alizarin yellow G have been investigated in buffered solution, in the pH range between 8.2 and 9.8. Complex formation was found to take place by two concurrent paths, one in which the rate of complex formation is independent of $[H^+]$ and one in which it is proportional to $[H^+]^{-1}$. The first path is ascribed to a reaction between Mg^{2+} and the monoprotonated form of the ligand, with a rate constant lower than the value for Mg^{2+} by a factor of at least 30. The second path can be ascribed to the reaction between Mg^{2+} and the unprotonated form of the ligand, with a normal rate constant. The possibility of a contribution of a reaction between $MgOH^+$ and the protonated ligand to this path is discussed. Both kinetic and spectrophotometric measurements show the existence of two complexes, one a chelate and one a complex in which the last proton is retained. The kinetic results were obtained by the temperature-jump method.

Introduction

Complex formation by substitution-labile cations as a rule takes place by the Eigen mechanism^{1,2} according to which the rate-determining step is water loss from the first coordination shell of the metal, after an ion pair between metal and ligand has been formed. The rate is thus characteristic for the cation and depends only on the charge, but not on the chemical nature of the ligand. Many protonated ligands react much more slowly and thus form exceptions to the rule,³⁻⁵ while the anion reacts at a normal rate. The effect is ascribed to an internal hydrogen bond blocking the reaction site. However, the mechanism by which these reactions take place, as well as the role of the protonated complex, has received little attention.

We have recently discussed⁶⁻⁸ the mechanism by which some of these internally hydrogen-bonded acids lose their proton to bases, reactions which again take place at an abnormally low rate. It seems interesting to try to draw parallels between the mechanism of proton loss and that of complex formation. In continuation⁵ of this plan, we have now investigated the mechanism of complex formation between Mg^{2+} and alizarin yellow G, which is



and will be abbreviated as HL^- .

Experimental Section

Magnesium nitrate, potassium nitrate, potassium hydroxide, nitric acid, and borax were analytical reagents. Triethanolamine (Riedel de Haen) and alizarin yellow G (Fluka) were used without further purification.

The Mg^{2+} concentration, a , was $(1-5) \times 10^{-3}$ M, in large excess over the ligand concentration b which was 10^{-4} M unless otherwise stated.

The ionic strength was 0.1 M throughout, regulated by the addition of potassium nitrate. The temperature was 25 °C.

The buffers were borax or triethanolamine. Duplicate series at pH 8.20 and 8.46 showed them to have no specific influence on the rate. (The buffer concentrations were $\leq 10^{-2}$ M; at concentrations higher than 2×10^{-2} M, an accelerating influence of borax starts to make itself felt.)

All kinetic results were obtained by the temperature-jump method. Each solution was "jumped" at least four times: the values of the reciprocal relaxation times exhibited a spread of $\pm 10\%$ at most, but usually much less. The mean value was adopted.

The pH was checked before and after the jump and was found to be stable within ± 0.01 unit of pH. We again⁶ assumed the pH to

be equal to $-\log a_{H^+}$ and calculated $[H^+]$ from $\gamma_{H^+} = 0.83$.

Blank tests in the absence of Mg^{2+} showed no signal in the time range of our experiments.

Relaxation times were evaluated manually as described previously.⁴ Calculations were carried out with a programmable minicomputer (CompuCorp Model 344).

Results

Spectrophotometric Results. Measurements were carried out at 360, 400, and 450 nm, with $b = 10^{-4}$, a varying between 1×10^{-3} and 10×10^{-3} M and pH varying between 8.0 and 9.2. (At higher values of pH, the change of absorbance with changing a became too small for reliable results to be obtained.) When $b/(A - \epsilon_{HL}b)$ (where A is the absorbance) was plotted against $1/a$ at constant pH, straight lines were obtained. An example at pH 8.46 and 450 nm is shown in Figure 1.

Kinetic Results. At given values of a , the reciprocal relaxation times $1/\tau$ increased markedly with increasing pH, and at constant pH, they were linear in a . These two effects are shown in Figure 2, for four values of pH. (Additional results, obtained at pH 8.20, 8.46, and 8.67, are not shown on this graph because, on the scale used, they would almost coincide with those obtained at pH 8.62.) We see that the increase of $1/\tau$ with increasing pH appears almost entirely in the slopes of this figure. The intercepts are little affected.

At pH 9.1, a change in b from 10^{-4} to 5×10^{-5} M was ascertained to have no influence on $1/\tau$.

Discussion

Equilibrium Constants. We can define an apparent equilibrium constant⁴

$$K_{app} = \frac{[\text{total complex}][H^+]}{[\text{total free metal ion}][\text{total free ligand}]} \\ = \frac{x[H^+]}{a(b-x)} \quad (1)$$

where we have made use of the inequalities $[L^-] \ll [HL^-]$, $[MgOH^+] \ll [Mg^{2+}]$, $b \ll a$. This leads to⁴

$$\frac{b}{A - b\epsilon_{HL}} = \frac{1}{\bar{\epsilon}_X - \epsilon_{HL}} + \frac{1}{\bar{\epsilon}_X - \epsilon_{HL}} \frac{[H^+]}{K_{app}a} \quad (2)$$

where $\bar{\epsilon}_X$ is the apparent extinction coefficient of the complex and may depend on pH.⁵ Equation 2 forms the basis of the graphs of the type of our Figure 1. At each pH, we obtain $K_{app}/[H^+]$ from the ratio of the intercept and the slope. If our complex were MgL , then K_{app} would be a true equilibrium

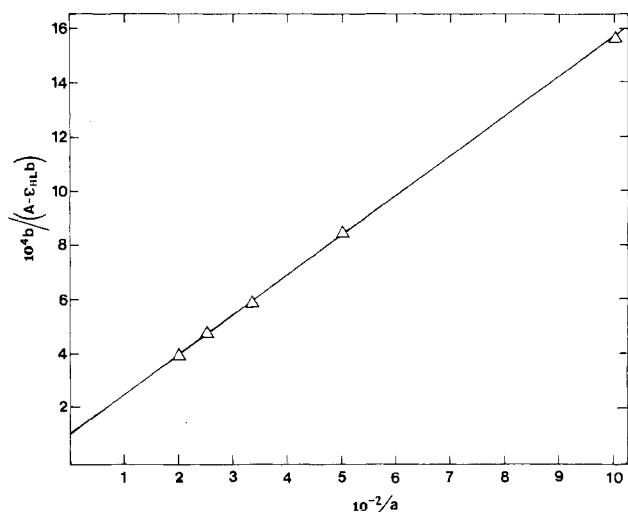


Figure 1. Value of $b/(A - \epsilon_{HL}b)$ as a function of $1/a$, at pH 8.46 and a wavelength of 450 nm (see eq 2).

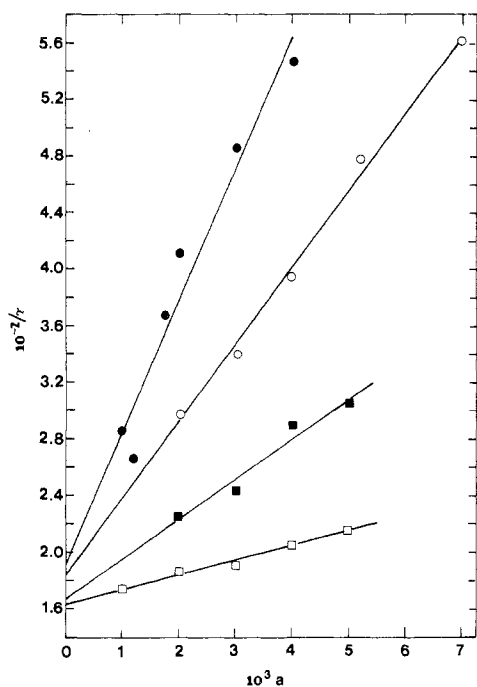
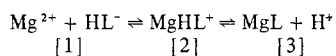


Figure 2. Reciprocal relaxation time as a function of $[\text{Ni(II)}]$: ●, pH 9.81; ○, pH 9.60; ■, pH 9.23; □, pH 8.62.

constant, independent of pH. Instead, our values for K_{app} increase with increasing $[\text{H}^+]$. This is shown in Figure 3 (circles) where the increase is seen to be linear. We conclude that two complexes must be present, according to



We then get

$$K_{app} = K_{13}(1 + K_{32}[\text{H}^+]) = K_{13} + K_{12}[\text{H}^+] \quad (3)$$

The slope and intercept of Figure 3 are thus equal to K_{12} and K_{13} , respectively. The presence of nonnegligible amounts of protonated complexes MHL where the chelate has not yet been formed has been previously assumed from kinetic evidence^{5,9-11} and from the results of spectrophotometric⁹ and polarographic¹² measurements and potentiometric titrations.¹²

Reaction Mechanism. A reaction scheme compatible with our kinetic results (Figure 2) together with the conclusions

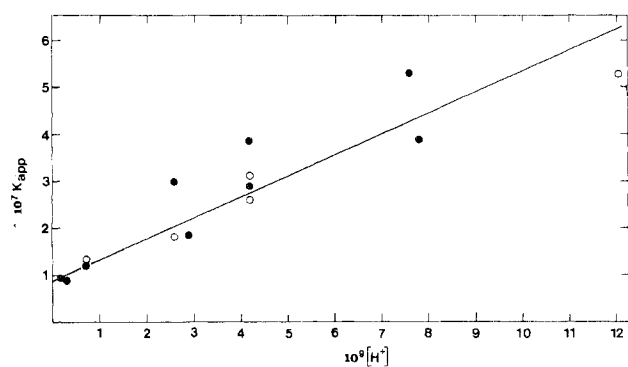


Figure 3. Dependence of K_{app} (as defined in eq 1) on $[\text{H}^+]$: ○, spectrophotometric results; ●, kinetic results.

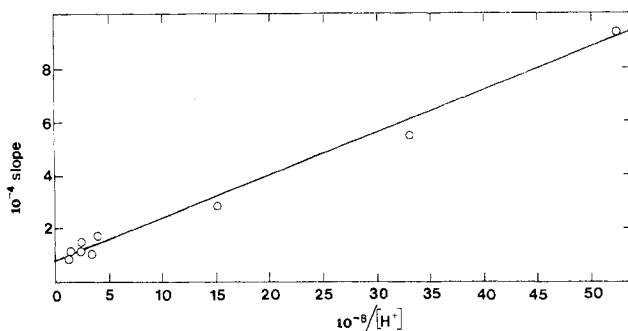
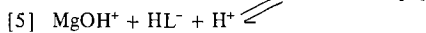
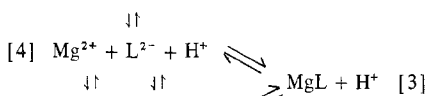
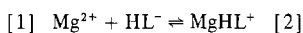


Figure 4. Values of $d(1/\tau)/da$ as a function of $[\text{H}^+]^{-1}$.

drawn from the spectrophotometric measurements is



Since the vertical, protolytic, equilibria are very fast, we expect to see only one relaxation time, given by

$$1/\tau = [k_{12} + k_{13} + (k_{43}K_a + k_{53}K_{\text{MgOH}})/[\text{H}^+]](a + [\text{H}^+]/K_{app}) \quad (4)$$

where K_a is the second dissociation constant of alizarin yellow G and K_{MgOH} is the hydrolysis constant of Mg^{2+} . A plot of the ratio between the slopes and intercepts of graphs of the type of Figure 2 as a function of $[\text{H}^+]$ thus provides an additional method for the evaluation of K_{13} and K_{12} . The results are shown as dots in Figure 3. The pH range is 8.2 to 9.8. (At lower pH the relaxation amplitudes became too small for satisfactory results to be obtained.) From Figure 3, using the combined kinetic and spectrophotometric results, we get $K_{13} = 8.50 \times 10^{-8}$ and $K_{12} = 44.6 \text{ M}^{-1}$ (calculated with the aid of a least-squares program which minimizes the sum of squares of $\ln K_{app} - \ln (K_{13} + K_{12}[\text{H}^+])$ in order to take account of the fact that the error in K_{app} is not constant, but is proportional to K_{app}). From these results we calculate that in the pH range between 8.0 and 9.8 the contribution of $[\text{MgHL}]$ decreases from almost 90% of the total complex concentration to ~9%.

The slopes of the $1/\tau$ vs. a plots (see Figure 2) are shown in Figure 4 as a function of $[\text{H}^+]^{-1}$. The intercept and slope of this figure are equal to $k_{12} + k_{13}$ and $k_{43}K_a + k_{53}K_{\text{MgOH}}$, respectively. However, in order to evaluate the rate constants from all of our 56 experiments, and not only from those carried out at seven constant values of pH, we transformed eq 4 into^{13,14}

$$1/\tau = [(k_{12} + k_{13})[\text{H}^+] + k_{43}K_a + k_{53}K_{\text{MgOH}}]B \quad (5)$$

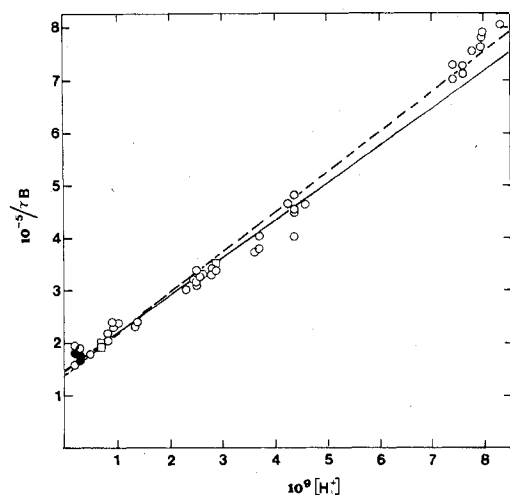


Figure 5. Values of $(1/\tau)/B$ as a function of $[H^+]$ (where B is defined by eq 6): broken line, "best line"; full line, obtained by minimizing $\sum \{\ln [(1/\tau)/B] - \ln [(k_{12} + k_{13})[H^+] + k_{43}K_a + k_{53}K_{MgOH}]\}^2$; points designated by squares represent two experiments each; the blackened area represents 11 experiments.

with

$$B \equiv a/[H^+] + 1/K_{app} \quad (6)$$

A plot of $(1/\tau)/B$ as a function of $[H^+]$ is shown in Figure 5. The best straight line is shown as a broken line. However, the error in the dependent variable is again proportional to the value of this variable; taking this into account as described above, we get the—only slightly different—full line. Its slope is equal to

$$k_{12} + k_{13} = 6.95 \times 10^3 \text{ M}^{-1} \text{ s}^{-1}$$

and its intercept to

$$k_{43}K_a + k_{53}K_{MgOH} = 1.53 \times 10^{-5} \text{ s}^{-1}$$

(If we had used Figure 3 for the calculation of the rate constants, the results would have been $(7.6 \pm 1.4) \times 10^3 \text{ M}^{-1} \text{ s}^{-1}$ and $(1.57 \pm 1.07) \times 10^{-5} \text{ s}^{-1}$, respectively. Figure 3 does not include *all* of our results but has the advantage of being independent of the values for K_{12} and K_{13} . The results are seen to be identical within less than one standard deviation.) If we neglect the contribution of the—somewhat unlikely—direct path $[1] \rightleftharpoons [3]$, we get from our equilibrium constants that

$$k_{21} = k_{12}/K_{12} = 156 \text{ s}^{-1}$$

Furthermore

$$k_{34} + k_{35} = (k_{43}K_a + k_{53}K_{MgOH})/K_{13} = 180 \text{ M}^{-1} \text{ s}^{-1}$$

Discussion of Rate Constants. Before discussing our rate constants, we have first to decide on the values which would be "normal" for a reaction between Mg^{2+} and ligands of our charge type, HL^- and L^{2-} , at $I = 0.1 \text{ M}$. From the results of an NMR measurement¹⁵ of the rate of exchange between bulk water and the inner coordination shell or Mg^{2+} , together with a statistical factor¹⁵ of 0.75 and together with the appropriate ion-pair constant (see, for instance, reference 2), we calculated that the rate constant should be $\sim 8 \times 10^5$ or $\sim 5 \times 10^6 \text{ M}^{-1} \text{ s}^{-1}$ for mono- or divalent normal ligands, respectively. Rate constants calculated from the values estimated by Eigen and Tamm¹⁶ for the rate-determining step in complex formation with various ligands are lower than this by a factor of ~ 4 . The discrepancy is ascribed by Neely and Connick¹⁵ to the

possibility of water being favored over other ligands in competing for the vacated coordination site. Experimental values^{3,4} concerning the rate of complex formation tend to confirm this view. They lie between the two extremes, but nearer the low than the high values. On this basis, we find that our value of k_{12} (or, possibly, $k_{12} + k_{13}$) for the reaction involving the monoprotonated ligand HL^- is lower than normal by a factor of at least 30 and not more than ~ 100 . Such lowered values are typical for internally hydrogen-bonded ligands.³⁻⁵ Again we see, in principle, two possible reaction paths which can explain the low value of the rate constant. According to one explanation, the reaction proceeds via *that* fraction of HL^- which is present in non-hydrogen-bonded, open form and can react by the usual Eigen mechanism. From the behavior of our ligand toward general bases⁸ we have recently concluded that this fraction is only about 1/300. Therefore, if this were the mechanism, the rate constant should be reduced to an even smaller value than we have found.

For this reason, we favor the second possibility according to which the Mg^{2+} must attack the hydrogen bond, either after the formation of an ion pair between metal and ligand or in a concerted, bimolecular step. The mechanism for the attack of Mg^{2+} on the reaction site is thus *different* from that assumed for bases⁸ and is similar to that of the reaction between Ni(II) and some substituted phenylazoresorcinols.⁵ It is interesting to note that the rate constants of Ni^{2+} and of the much more substitution-labile Mg^{2+} are reduced below their normal values by similar factors (≥ 30 in the present case and 20–100 in the case of Ni^{2+} and three phenylazoresorcinols).

Let us now consider the complex formation via the $[H^+]^{-1}$ -dependent path. There is no possibility⁵ to separate the contribution of pathways $[4] \rightleftharpoons [3]$ and $[5] \rightleftharpoons [3]$. If we ascribe the observed rate *entirely* to the reaction $[4] \rightleftharpoons [3]$, we get (using¹⁷ $K_a = 8.3 \times 10^{-12} \text{ M}$) $k_{43} = 1.84 \times 10^6 \text{ M}^{-1} \text{ s}^{-1}$ which is a normal value for a reaction involving a divalent ligand.

Nevertheless, a contribution of the pathway $[3] \rightleftharpoons [5]$ cannot be excluded. True, nothing seems to be reported about an enhancement of the rate of water exchange by the presence of OH^- in the inner coordination sphere of Mg^{2+} —in contradistinction with ions of the type of Fe(III).¹ But very little enhancement is needed for the reaction $[3] \rightleftharpoons [5]$ to make itself felt. If the *entire* $[H^+]^{-1}$ -dependent reaction were due to this path, then (using¹⁸ $[MgOH^+]/[Mg^{2+}][OH^-] \approx 250 \text{ M}^{-1}$ and¹⁹ $K_w = 1.58 \times 10^{-14} \text{ M}$) we should get $k_{53} = 3.9 \times 10^6 \text{ M}^{-1} \text{ s}^{-1}$.

A value of k_{53} of $\sim 10^6 \text{ M}^{-1} \text{ s}^{-1}$ would therefore suffice for this reaction to make an appreciable contribution. The difference between Mg^{2+} and $MgOH^+$ in their reaction with HL^- would then lie in the fact that the strong base $MgOH^+$ is much more efficient than Mg^{2+} in opening the hydrogen bond,⁸ and water loss takes over as the rate-determining step.

An exactly analogous case may be made for the participation of a reaction between $MgOH^+$ and the monoprotonated ligand in the case of eriochrome black T, a possibility which had not been considered at the time.⁴

In order to explain the pH dependence of the reaction between Ni(II) and substituted phenylazoresorcinols,⁵ in a pH range where the relative concentration of the unprotonated ligand is negligibly small, we have recently brought forward a similar argument in favor of the enhanced reactivity of $NiOH^+$ over Ni^{2+} toward internally hydrogen-bonded ligands.

Registry No. Mg^{2+} , 22537-22-0; HL^- , 61009-70-9.

References and Notes

- M. Eigen and G. Wilkins, *Adv. Chem. Ser.*, No. 49, 55 (1965).
- K. Kustin and J. Swinehart, *Prog. Inorg. Chem.*, **13**, 107 (1970).
- D. N. Hague and M. Eigen, *Trans. Faraday Soc.*, **62**, 1236 (1966).

- (4) R. Koren, B. Perlmutter-Hayman, and R. Shinar, *Int. J. Chem. Kinet.*, **6**, 39 (1974).
 (5) B. Perlmutter-Hayman and R. Shinar, *Inorg. Chem.*, **15**, 2932 (1976).
 (6) B. Perlmutter-Hayman and R. Shinar, *Int. J. Chem. Kinet.*, **7**, 453, 798 (1975).
 (7) B. Perlmutter-Hayman, R. Sarfaty, and R. Shinar, *Int. J. Chem. Kinet.*, **8**, 741 (1976).
 (8) B. Perlmutter-Hayman and R. Shinar, *Int. J. Chem. Kinet.*, in press.
 (9) B. Perlmutter-Hayman and R. Shinar, *Isr. J. Chem.*, in press.
 (10) W. A. Johnson and R. G. Wilkins, *Inorg. Chem.*, **9**, 1917 (1970).
 (11) D. W. Margerum, D. B. Rorabacher, and J. F. G. Clarke, Jr., *Inorg. Chem.*, **2**, 667 (1963).
 (12) P. H. Tedesco and J. A. Gonzalez Quintana, *J. Inorg. Nucl. Chem.*, **37**, 1798 (1975).
 (13) F. P. Cavasino, *Ric. Sci., Parte 2: Sez. A*, **8**, 1120 (1965); F. P. Cavasino, *J. Phys. Chem.*, **69**, 4380 (1965).
 (14) B. Perlmutter-Hayman, *Adv. Mol. Relaxation Processes*, in press.
 (15) J. Neely and R. Connick, *J. Am. Chem. Soc.*, **92**, 3476 (1970).
 (16) M. Eigen and K. Tamm, *Z. Elektrochem.*, **66**, 107 (1962).
 (17) M. C. Rose and J. E. Stuehr, *J. Am. Chem. Soc.*, **94**, 5532 (1972).
 (18) L. G. Sillen and A. E. Martell, *Chem. Soc., Spec. Publ.*, No. **17** (1964); No. **25** (1971).
 (19) H. S. Harned and B. B. Owen, "The Physical Chemistry of Electrolytic Solutions", 2d ed, Reinhold, New York, N.Y., 1950, p 485.

Contribution from the Department of Chemistry,
 University of California, Santa Barbara, California 93106

Reactivity of Metal Radicals Generated Photochemically. Effects of Solvent and of Trapping Agent Concentrations on Quantum Yields for Photolysis of Hexacarbonylbis(π -cyclopentadienyl)ditungsten(I), $[\pi\text{-CpW}(\text{CO})_3]_2^1$

RICHARD M. LAINE and PETER C. FORD*²

Received August 9, 1976

AIC60583V

The metal radical $\pi\text{-CpW}(\text{CO})_3$, generated by the 520-nm photolysis of $[\pi\text{-CpW}(\text{CO})_3]_2$, displays considerable selectivity in its reactions with various chlorocarbon trapping agents in solution. As reported previously, the principal metal-containing photolysis product is $\pi\text{-CpW}(\text{CO})_3\text{Cl}$ which results from the abstraction of chlorine from the chlorocarbon; however, another low-yield photodecomposition pathway is also evident in the absence of trapping agent. The sensitivity of the metal radical toward trapping agent follows the order $\text{CCl}_4 \gg \text{CHCl}_3 > \text{PhCH}_2\text{Cl} \gg \text{CH}_2\text{Cl}_2$ in a manner consistent with the reactivities of other radicals. The effects of lamp intensity and of trapping agent concentrations on quantum yields are reported and a kinetic scheme consistent with these results is proposed. In addition, quantum yields are reported for the reactions in carbon tetrachloride, chloroform, and dichloromethane as solvents, and it is noted that these values do not simply parallel the reactivities of the trapping agents but must reflect solvent effects on primary quantum yields for formation of the metal radicals.

Photolytic generation of reactive organometallic radicals has received considerable attention in the recent literature.³⁻⁶ The interest in such species derives in part from the potential roles of metal radicals in the synthesis of new organometallic complexes (especially mixed polynuclear species),³ in mechanisms of oxidative addition,^{7,8} in metal carbonyl substitution reactions,^{9,10} and in certain homogeneous catalysis processes.^{6,11,12} Thus it is of interest to examine the reaction dynamics of photolytically generated metal radicals. Photolysis of neutral bimetallic complexes such as $[\pi\text{-CpW}(\text{CO})_3]_2$ and $[\pi\text{-CpMo}(\text{CO})_3]_2$ leads to homolytic metal-metal bond cleavage to give such species.^{4,5} Reported here is a study of the reactions of the photolytically generated metal radical $\pi\text{-CpW}(\text{CO})_3$ with a variety of chlorocarbon trapping agents as neat solvents and in tetrahydrofuran solution.

Experimental Section

Materials. Spectroscopic grade solvents were used. Chlorocarbon solvents and trapping agents were stored in the dark over molecular sieves and distilled in a nitrogen atmosphere immediately prior to use. Tetrahydrofuran (THF) was distilled from sodium benzophenone ketyl under nitrogen immediately prior to use. Hexane was stored over P_2O_5 and distilled under nitrogen prior to use. Manipulations of air-sensitive complexes were carried out under a nitrogen atmosphere. $[\pi\text{-CpW}(\text{CO})_3]_2$ is an air- and light-sensitive compound; however, the following synthesis procedure gave pure material. To 20 ml of freshly distilled THF were added 0.036 g (1.5×10^{-3} mol) of NaH and 0.55 g (1.65×10^{-3} mol) of $\pi\text{-CpW}(\text{CO})_3\text{H}$. The mixture was stirred magnetically until hydrogen evolution ceased. A 0.65-g (1.4×10^{-3} mol) portion of $\pi\text{-CpW}(\text{CO})_3\text{I}$ was added, the solution was stirred for 5 h and then was refluxed for 40 h. After the solution was allowed to cool to room temperature, 2 ml of acetic acid was added and the mixture was stirred for 1 h. The solvent and excess acetic acid were removed by high-vacuum evaporation, and then unreacted

$\pi\text{-CpW}(\text{CO})_3\text{H}$ was sublimed from the remaining material (60 °C at ~ 0.1 mmHg). Following the sublimation, the remaining residue was extracted with dichloromethane and filtered in a dark room. The $[\pi\text{-CpW}(\text{CO})_3]_2$ was precipitated from the deep red solution by addition of hexane. Recrystallization from dichloromethane in the dark gave 0.75 g (68% yield) of crystalline $[\pi\text{-CpW}(\text{CO})_3]_2$ with IR, UV, and mass spectral properties closely matching the literature values.^{3,13} $\pi\text{-CpW}(\text{CO})_3\text{Cl}$ and $\pi\text{-CpW}(\text{CO})_3\text{I}$ were prepared from $\pi\text{-CpW}(\text{CO})_3\text{H}$ by the literature procedures¹⁴ and were recrystallized from dichloromethane/hexane in the dark.

Photolysis Procedures. Solutions of THF, with or without measured quantities of trapping agent, were placed in a small Schlenk tube and degassed via three freeze-thaw cycles. Nitrogen was reintroduced, $[\pi\text{-CpW}(\text{CO})_3]_2$ was added, and the resulting homogeneous solution was transferred by syringe to an airtight 2-cm quartz photolysis cell previously purged with nitrogen. The initial spectrum was recorded on a Cary 14 spectrophotometer. In most cases the initial solutions were relatively optically dense ($\text{OD} > 0.5$) at the irradiation wavelength. The cell was then placed in a thermostated compartment of the photolysis train equipped with a 150-W xenon short-arc lamp with interference filters of 520 or 460 nm for wavelength selection. Actinometry at each wavelength was accomplished using Reinecke's salt. The infrared solution spectra of reactants and products were recorded on a Perkin-Elmer Model 225 grating infrared spectrophotometer.

Results

The electronic spectrum of $[\pi\text{-CpW}(\text{CO})_3]_2$ (A) displays two absorption bands in the near-UV-visible region. These are relatively insensitive to the solvent and in CCl_4 have absorption maxima at 493 and 362 nm (ϵ 3.05×10^3 and $2.29 \times 10^4 \text{ M}^{-1} \text{ cm}^{-1}$, respectively) which have been assigned as $\pi \rightarrow \sigma^*$ and $\sigma \rightarrow \sigma^*$ transitions of the metal-metal bond.⁴ Photolysis of A with 520-nm light in chlorocarbon solvent leads to a product identified from its IR and electronic spectrum